A mesh-free Darwin model for non-radiative plasma simulation

<u>M. Mašek</u>[1], P. Gibbon[1]

[1] *John von Neumann Institute for Computing, ZAM, Forschungszentrum Jülich GmbH,*
D-52425 Jülich, Germany

A new type of mesh-free plasma simulation model is presented, capable of modelling particle systems with slowly varying magnetic and electric fields within the Darwin or magnetoinductive approximation. The model is implemented within the code framework PEPC (Pretty Efficient Parallel Coulomb-solver), which is based on an O($N \log N$) Barnes-Hut tree algorithm [1, 2]. The efficient scaling properties of this algorithm already permit multi-million charged-particle simulations to be performed on modern computer architectures, offering new possibilities for modelling large-scale magnetised plasmas.

The Darwin model

The Darwin, or magnetoinductive approach to kinetic plasma modelling is an attractive technique for relaxing timestep constraints in physical situations where electromagnetic radiation can be neglected. On a standard spatial grid, solving the Maxwell field equations becomes subject to the CFL condition $\Delta t < \Delta x/c$, ensuring that the fastest vacuum modes are properly resolved. Dispensing with these modes therefore allows larger timesteps to be used, potentially leading to a more efficient numerical solution of the problem at hand. Technically this is achieved by using a modified set of Maxwell's equations in which the transverse displacement current is omitted in Ampere's law, leaving a system of equations valid to order v^2/c^2 and allowing the plasma particles to interact with slowly-varying, self-generated fields [3, 4].

The starting point is the Darwin Lagrangian for a system of mutually interacting particles with coordinates $\vec{r}_i$ and velocities $\vec{v}_i$ [5, 6]:

$$L = -\frac{1}{2} \sum_i m_i c^2 \sqrt{1 - \frac{v_i^2}{c^2}} - \frac{1}{2} \sum_i q_i \phi_i + \frac{1}{2} \sum_i \frac{q_i}{c} \vec{v}_i \cdot \vec{A}_i, \tag{1}$$

where ϕ_i and $\vec{A}_i$ are the scalar and vector potentials obtained from the particle distribution (exluding external fields). Although not strictly consistent with the $O(v^2/c^2)$ approximation made in neglecting retardation, we keep the fully relativistic expression for the free particle component. This allows us to recover the usual Lorentz momentum equation from the Euler-Lagrange equations

$$\frac{d\vec{P}_i}{dt} = \frac{\partial L}{\partial \vec{r}_i} \tag{2}$$

where

$$\vec{P}_i \equiv \frac{\partial L}{\partial \vec{v}_i} = m_i \vec{v}_i + \frac{q_i}{c} \vec{A}_i \tag{3}$$

is the canonical momentum of a single particle. The Lagrangian in Eq. (1) has an associated Hamiltonian given by:

$$\begin{aligned} H &\equiv \sum \vec{P}_i \cdot \vec{v}_i - L \\ &= \sum \gamma_i m_i c^2 + \frac{1}{2} \sum_i q_i \phi_i + \frac{1}{2} \sum_i \frac{q_i}{c} \vec{v}_i \cdot \vec{A}_i. \end{aligned} \tag{4}$$

where $\gamma_i = (1 - v_i^2/c^2)^{-1/2}$. Because the Lagrangian does not depend explicitly on time, we immediately obtain an energy conservation relation $dH/dt = 0$.

The potentials and fields for this system of particles are given by:

$$\phi_i(\vec{r}_i) = \sum_{j \neq i} \frac{q_j}{r_{ij}}, \tag{5}$$

$$\vec{E}_i^l(\vec{r}_i) = \sum_{j \neq i} \frac{q_j \vec{r}_{ij}}{r_{ij}^3}, \tag{6}$$

$$\vec{A}_i(\vec{r}_i) = \frac{1}{2c} \sum_{j \neq i} \frac{q_j \vec{v}_j}{r_{ij}} + \frac{1}{2c} \sum_{j \neq i} \frac{(q_j \vec{v}_j \cdot \vec{r}_{ij}) \vec{r}_{ij}}{r_{ij}^3}, \tag{7}$$

$$\vec{B}_i(\vec{r}_i) = \nabla \times \vec{A}_i = \frac{1}{c} \sum_{j \neq i} \frac{q_j \vec{v}_j \times \vec{r}_{ij}}{r_{ij}^3}, \tag{8}$$

$$\vec{E}_i^t(\vec{r}_i) = -\frac{1}{c} \frac{\partial \vec{A}_i}{\partial t} = -\frac{1}{2c^2} \sum_{j \neq i} \frac{q_j \dot{\vec{v}}_j}{r_{ij}} - \frac{1}{2c^2} \sum_{j \neq i} \frac{(q_j \dot{\vec{v}}_j \cdot \vec{r}_{ij}) \vec{r}_{ij}}{r_{ij}^3}, \tag{9}$$

where $\vec{r}_{ij} = \vec{r}_i - \vec{r}_j$. Note that all of these quantities are expressed as moments of the particle distribution $\{\vec{r}_i, \vec{v}_i, \dot{\vec{v}}_i\}$, and do not require explicit time-differencing. This approach circumvents the stability and boundary problems normally associated with PIC- or Vlasov-based Darwin models because all field quantities are automatically expressed in terms of the particle moments [4]. The Lorentz momentum equation including both internal and external fields is

$$\frac{d}{dt}(\gamma_i \vec{v}_i) = \frac{q_i}{m_i}(\vec{E}_i^l + \vec{E}_i^t + \frac{\vec{v}_i}{c} \times \vec{B}_i) + \frac{q_i}{m_i} \vec{F}_i^{ext} \tag{10}$$

Multipole expansion, Barnes-Hut tree algorithm

The present model is entirely gridless and the fields governing self-consistent particle motion are computed from the particle position, velocities and accelerations. It is analogous to the standard molecular dynamics approach, which is normally prohibitively expensive, requiring $O(N^2)$ operations for the field evaluation at each iteration. However, by employing multipole expansions of the fields via a hierarchical tree algorithm, this computational effort can be reduced to a more managable $O(N \log N)$. In the present model the electrostatic field is expanded up to the fourth order, while for the magnetic field and the vector potential an expansion up to the second order is used. This combination ensures a reasonable trade-off between force accuracy and CPU time. The multipole expansion of expressions (5)-(9) is a straightforward exercise, which to quadrupole and dipole order for the irrotational and solenoidal fields respectively, yields:

$$\phi(\vec{R}) = \sum_j \frac{q_j}{R} + \sum_j \frac{q_j \vec{r}_j \cdot \vec{R}}{R^3} + \frac{1}{2} \sum_j \left(-\frac{q_j r_j^2}{R^3} + \frac{3 q_j \vec{R} \cdot \vec{r}_j \vec{r}_j \cdot \vec{R}}{R^5} \right) + O(R^{-4}), \tag{11}$$

$$\vec{E}^l(\vec{R}) = \sum_j \frac{q_j \vec{R}}{R^3} + \sum_j \frac{q_j \vec{r}_j}{R^3} - \sum_j \frac{q_j (\vec{r}_j \cdot \vec{R}) \vec{R}}{R^5} - \frac{3}{2} \sum_j \frac{q_j r_j^2 \vec{R}}{R^5}$$

$$- 3 \sum_j \frac{q_j (\vec{r}_j \cdot \vec{R}) \vec{r}_j}{R^5} + \frac{15}{2} \sum_j \frac{q_j (\vec{R} \cdot \vec{r}_j)(\vec{r}_j \cdot \vec{R}) \vec{R}}{R^7} + O(R^{-5}), \tag{12}$$

$$\vec{A}(\vec{R}) = \frac{1}{2c} \sum_j \frac{q_j \vec{v}_j}{R} + \frac{1}{2c} \sum_j \frac{(q_j \vec{v}_j \cdot \vec{R}) \vec{R}}{R^3} + \frac{1}{2c} \sum_j \frac{\vec{m}_j \times \vec{R}}{R^3}$$

$$- \frac{1}{2c} \sum_j \frac{(q_j \vec{v}_j \cdot \vec{r}_j) \vec{R}}{R^3} + \frac{3}{2c} \sum_j \frac{(q_j \vec{v}_j \cdot \vec{R})(\vec{r}_j \cdot \vec{R}) \vec{R}}{R^5} + O(R^{-3}), \tag{13}$$

$$\vec{B}(\vec{R}) = \frac{1}{c}\sum_j \frac{q_j\vec{v}_j\times\vec{R}}{R^3} + \frac{1}{c}\sum_j \frac{\dot{\vec{m}}_j}{R^3} + \frac{3}{c}\sum_j \frac{(q_j\vec{v}_j\times\vec{R})(\vec{R}\cdot\vec{r}_i)}{R^5} + O(R^{-4}), \qquad (14)$$

$$\vec{E}^t(\vec{R}) = -\frac{1}{2c}\sum_j \frac{q_j\dot{\vec{v}}_j}{R} - \frac{1}{2c}\sum_j \frac{(q_j\dot{\vec{v}}_j\cdot\vec{R})\vec{R}}{R^3} - \frac{1}{2c}\sum_j \frac{\dot{\vec{m}}_j\times\vec{R}}{R^3}$$

$$+\frac{1}{2c}\sum_j \frac{(q_j\dot{\vec{v}}_j\cdot\vec{r}_j)\vec{R}}{R^3} - \frac{3}{2c}\sum_j \frac{(q_j\dot{\vec{v}}_j\cdot\vec{R})(\vec{r}_j\cdot\vec{R})\vec{R}}{R^5} + O(R^{-3}), \qquad (15)$$

where $\vec{R}$ is a vector connecting the test particle and the centre of charge of faraway particle cloud and $\vec{r}_j$ is the separation of centre of charge and individual particle in the cloud ($r_j << R$).

To decide how to group more distant particles together into a pseudoparticle the Barnes Hut method is employed. This uses a criterion

$$s/d < \theta, \qquad (16)$$

where s is 'size' of node (or twig), d is a distance between particle and centre of charge of pseudoparticle and θ is a fixed tolerance parameter. When this criterion is fulfilled, the internal structure of pseudoparticle is ignored and its multipole moments are added to the cumulative force for that particle. Otherwise, the node is subdivided as long as the relation (16) is fulfilled. A high accuracy is achieved with a small value of θ, but this is paid for with a longer computation time. (In the limit $\theta \to 0$ every pair interaction is computed with computational effort $O(N^2)$ as in standard molecular dynamics). In practice, a good compromise between rapid and accurate force calculation typically lies in the interval $\theta \sim 0.3 - 0.7$.

Preliminary tests

In order to test the Darwin model implemented within the PEPC, we chose a simple example of an electron beam propagating through vacuum in the absence of external fields. This case is solvable analytically within the paraxial approximation. The envelope equation describing the time evolution of the particle beam radius is given by [7]:

$$\ddot{R} - \frac{U_b}{\beta^2\gamma^2 R} = \frac{\left[R^2[V^2 - (\dot{R})^2]\right]_{t=t_0}}{R^3}, \qquad (17)$$

where $U_b = \frac{q\beta c\mu_0 I_b}{4\pi\gamma m}$ characterizes self-consistent electromagnetic field of beam comprising particles with charge q, mass m and longitudinal velocity $\beta = v/c$; $\gamma = (1-\beta^2)^{-1/2}$. $R^2 = \frac{1}{N}\sum r_i^2$ and $V^2 = \frac{1}{N}\sum v_i^2$ are the mean square radius and the mean square transverse velocity of the beam respectively. For detailed information see Ref. [7].

Figure 1: Temporal dependence of rms beam radius obtained from the numerical simulation compared to result of analythical envelope model ($N_e = 70,000$, $r_b = 2.5$, $u = \gamma v = 0.8$, $\theta = 0.5$).

To compare results of the PEPC code with the analytical theory above, we carried out several runs using a beam containing 70,000 particles. The initial longitudinal velocity of the electron
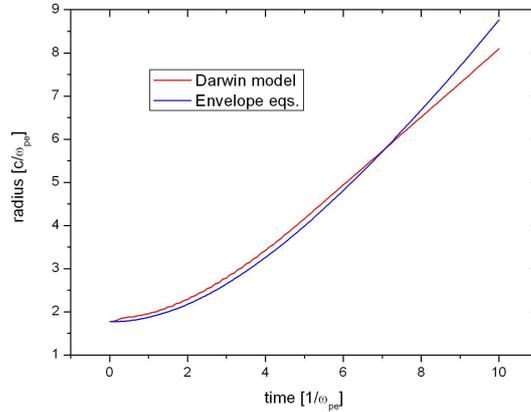
beam was chosen as $u/c = \gamma\beta = 0.8$ and θ was set to 0.5. Results obtained from the numerical simulation using Darwin model are compared to the solution of the envelope equation in Fig. 1. Considering that the beam is slightly accelerated in longitudinal direction due to the non-zero electrostatic force on particles at the edges of beam, we find a good agreement between these models. The envelope model based on the single-particle equation of motion does not take into account changes in beam velocity nor changes in the self-pinching magnetic field, which in reality increases and causes a slower radial expansion of beam. If we made these corrections to the envelope model, we should obtain the same asymptotic behaviour as for the full Darwin model.
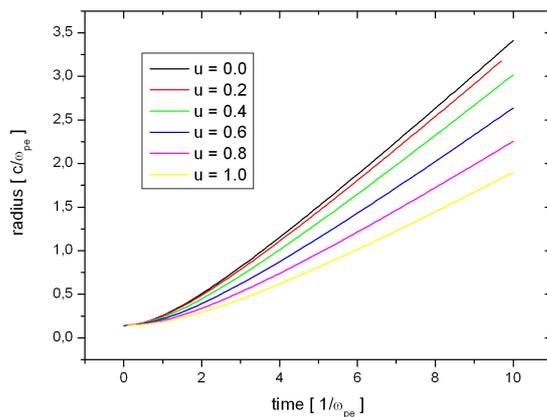

Figure 2: Comparison of beam expansion for several different initial velocities, demonstrating the influence of self-generated magnetic field on the beam.

Another set of test runs was carried out to determine the influence of beam velocity on the temporal evolution of beam radius. In these simulations we used 10,000 particles forming a beam with length $L_b = 5.0$ and radius $r_b = 0.2$. Results are shown in Fig. 2. As expected, with increasing beam velocity the radial magnetic field increases as well. This self-pinching magnetic field slows down the beam radial expansion.

Conclusion

We have demonstrated a new type of mesh-free magnetoinductive (Darwin) plasma simulation model. Using a the simple test case of a relativistic particle beam, we have shown good agreement between the code and analytical theory in certain limiting cases. Future work will focus on applying this new model to more complex beam transport phenomena, such as fast electron flow in laser plasma interactions.

Acknowledgement

References

[1] P. Gibbon, F. N. Beg, E. L. Clark, R. G. Evans, and M. Zepf, Phys. Plasmas, **11** (2004), 4032.

[2] http://www.fz-juelich.de/zam/pepc

[3] A. N. Kaufmann, P. S. Rostler, Phys. Fluids **14** (1971), 446–448.

[4] D. W. Hewett, Space. Sci. Rev. **42** (1985), 29–40.

[5] C. G. Darwin, Phil. Mag. **39** (1920), 537.

[6] L. D. Landau, L. M. Lifshitz, L. P. Pitaevskii, *Electrodynamics of Continuous Media*, 2nd Edition, Pergamon, New York, 1984.

[7] E. P. Lee, and R. K. Cooper, Particle Accelerators, **7** (1976), 83–95.